scientific reports

Check for updates

OPEN

Coupled power generators require stability buffers in addition to inertia

Gurupraanesh Raman[1,2,3], Gururaghav Raman[1,2,3] & Jimmy Chih-Hsien Peng[1]✉

Increasing the inertia is widely considered to be the solution to resolving unstable interactions between coupled oscillators. In power grids, Virtual Synchronous Generators (VSGs) are proposed to compensate for reducing inertia as rotating fossil-fuel-based generators are being phased out. Yet, modeling how VSGs and rotating generators simultaneously contribute energy and inertia, we surprisingly find that instabilities of a small-signal nature could arise despite fairly high system inertia if the generators' controls are not coordinated at the system level. Importantly, we show there exist both an optimal and a maximum number of such VSGs that can be safely supported, a previously unknown result directly useful for power utilities in long-term planning and prosumer contracting. Meanwhile, to resolve instabilities in the short term until system-level coordination can be achieved, we argue that the new market should include another commodity that we call stability storage, whereby—analogous to energy storage buffering energy imbalances—VSGs act as decentralized stability buffers. While demonstrating the effectiveness of this concept for a wide range of energy futures, we provide policymakers and utilities with a roadmap towards achieving a 100% renewable grid.

Power grids around the world are transitioning from conventional fossil-fuel-based generation to renewables such as solar photovoltaic and wind generation in a bid to combat climate change. This has ushered in an era where the dominant share of electricity generation may no longer come from large rotating synchronous machines, but rather, smaller power electronic converters—called inverters—that transfer DC power from the renewables into the AC power grid. A key consequence of replacing synchronous generation by inverters is the reduction in the grid inertia, which has heretofore existed in the form of the inherent kinetic energy in the spinning rotors[1,2]. When inertia becomes insufficient, small power disturbances in the power grid result in larger frequency deviations, which when exceeding allowable limits, can trip generators and cause blackouts[3]. Cognizant of this, many grid operators around the world (e.g., in Hawaii[4], Puerto Rico[4], United Kingdom[5], Europe[6]) find that inverters need to start contributing inertia in the near future, considering different energy futures and approaches to decarbonization within and across nations. Such inverters would be different from the overwhelming majority of inverters in the present that simply inject renewable power to support the grid (i.e., operate in the *grid-following mode*): they would actively control the voltage and frequency of the grid (i.e., operate in the *grid-forming mode*). Effectively, they would operate as Virtual Synchronous Generators (VSGs) to emulate the inertial dynamics of their rotating counterparts, and are planned to be incentivized for this service through a new stability market (e.g., see ref.[7] for the UK).

As yet, VSGs have not been implemented in bulk power grids at any scale, and there are no operational standards as to how systems with both rotating and virtual synchronous generators should be operated, especially as their relative shares change in the future[8]. Motivated by this lack of industry experience with VSGs and given their imminent introduction in grids around the world, we ask the question: is maintaining adequate inertia alone sufficient for maintaining the stability of the grid, for the entire range of expected energy futures? In studying the stability implications of an inertia market, we model how energy will be shared amongst the synchronous generators and the VSGs. The manner in which they do this and respond simultaneously in real time governs the system's *small-signal stability*, a critical measure of how quickly incremental power disturbances are damped out. The small-signal stability is influenced strongly by the control parameters of the generators (rotating or virtual), as well as the inertia. Nevertheless, there are no comprehensive studies in the literature focusing on the nexus

[1]Department of Electrical and Computer Engineering, National University of Singapore, 2 Engineering Drive 3, Singapore 117581, Singapore. [2]Singapore-ETH Centre, Future Resilient Systems, CREATE campus, 1 CREATE Way, #06-01 CREATE Tower, Singapore 138602, Singapore. [3]These authors contributed equally: Gurupraanesh Raman and Gururaghav Raman. ✉email: jpeng@nus.edu.sg

between inertia, energy sharing amongst the various generators, and small-signal stability. Such a study is in fact essential as VSGs are introduced in the grid due to two factors. First, VSGs are operated by prosumers—entities who consume and produce electricity at the same time—who may flexibly connect, disconnect, or operate their inverters to satisfy their own financial ends in a deregulated environment rather than being concerned with global stability, which they have no awareness of. Second, the inverters are located at the grid edge rather than in a few centralized locations as the synchronous generators were, rendering real-time control unscalable[9].

With this in mind, we take the power grid of the Greater London area, and analyze its small-signal stability for various energy futures forecast by the grid operator, National Grid. Surprisingly, we demonstrate that the grid can become unstable even at high inertia levels and low shares of inverter generation when the VSGs are not properly sized. We further show that for a given inertia level, there exists an optimal as well as a maximum number of VSGs that can be incorporated safely into the grid. In doing so, we effectively provide a long-term roadmap for energy policymakers and utilities in planning the required inertia, and the number and capacity of the VSGs for each energy future. While the results shown here are for the Greater London network, the trends are explained by control-theoretic concepts and are therefore applicable to other grids as well. Next, we show that to guarantee the stability in the short term, the VSGs themselves must necessarily participate in stabilizing the grid and that external interventions are not successful. To realize this, we view small-signal stability as a decentralized and additive resource that can be commoditized through what we call *stability storage*, so that it can also be traded in the stability market. Drawing inspiration from the well-known use of energy storage to mitigate generation-demand imbalances in a decentralized manner[10], we demonstrate that having stability storage can effectively solve the instability problem.

Broadly, VSGs have the ability to enable grids with 100% renewable generation, and are crucial for achieving a sustainable electric grid in nations that do not have appreciable hydro or geothermal potential. Therefore, although our study appears to arise from a control perspective, the answers—which define the operational philosophy of future power grids worldwide—govern the smooth transition towards sustainability.

Related works

AC power grids with synchronized generators are complex systems exhibiting a variety of instability phenomena that are of interest to both power engineers[3,11–14] and network scientists[15–21]. Specific to the oscillatory dynamics of generators presently under consideration, our work differs from previous studies in two substantive ways. First, previous studies have focused on the modeling of VSGs[22–26] and examined[3,12,13,17,19] the impact of generator controller parameters and network interconnections on the ability of generators to self-synchronize, in other words, to preserve small-signal stability in the grid. In particular, the positive impact of higher inertia on the small-signal stability has been reported in ref.[14,17,18], highlighting the need for VSGs in future power grids. Nevertheless, an unanswered question remains as to how many inverters should participate as VSGs—contributing both inertia as well as power—and what (if any) is the limit on this number. The challenge here is that when considerations of inertia and power sharing are combined, there is no degree of freedom in the primary controller parameters whereby they can be tuned to improve stability; see "Methods". Second, common to the prior studies is that they have treated small-signal stability as a global measure, and not as a distributed commodity that can be provided by multiple grid-edge devices in an additive manner. As such, small-signal stability has never been commoditized for provision through a market, let alone in the context of VSGs. Our paper demonstrates how this can be done using virtual impedance control, a well known stabilizing strategy[27–30].

There is another body of literature focused on developing control solutions for grid-forming inverters that result in grids that are theoretically stable for any configuration, e.g., by using lead-lag compensators[31,32], measurement frame rotation[33], etc. However, such stability guarantees do not hold when synchronous generators and inverters are both present, or when the latter have heterogeneous control strategies[34]. Given that in practice, inverters and synchronous generators are likely to co-exist, and that inverters are likely to come from different vendors and have different operational constraints specified by their individual prosumer operators[35], these control solutions may not sufficiently ensure the robustness of the future grid. Centralized coordination, however, is not a scalable alternative given the number and dispersed nature of the generators[36]; an alternate decentralized market-based approach is proposed here. We mention that while our focus is only on grid-forming inverters, some energy markets presently do allow grid-following inverters to provide inertia (called fast frequency response). However, we do not consider these in our analyses due to three reasons: (i) their response time is too slow for this service alone to be adequate without grid-forming inverters[2,37]; (ii) following their inertial response, they may suffer from an energy-recovery phase that lowers the frequency again, particularly in the case of wind generation[37]; and (iii) such grid-following inverters do not affect the small-signal stability of the grid without additional active damping controls[38].

Results and discussion

Inertia - small-signal stability nexus. To evaluate the stability of the power grid when VSGs provide power and inertia in tandem with rotating generators, we use the distribution grid of Greater London as a case study. We consider four future energy scenarios developed by the system operator, National Grid, to represent the range of credible futures for the UK energy system to achieve full decarbonization by 2025[41]. These scenarios include projections[39] of the system inertia, which are shown in Fig. 1a. Additionally, we obtain projections for the average System Non-Synchronous Penetration (SNSP)[40], which is the overall share of the power supplied by inverter-based generators. Finally, we derive the grid topology using publicly available data, simulate the system for different inertia and SNSP projections, and examine the small-signal stability at each step; see "Methods". The latter is quantified by the damping ratio of the least stable non-zero eigenmode, a fraction that varies between $[-1, 1]$—the grid is more stable if it is positive and closer to 1, and more unstable if it is negative and closer to -1.

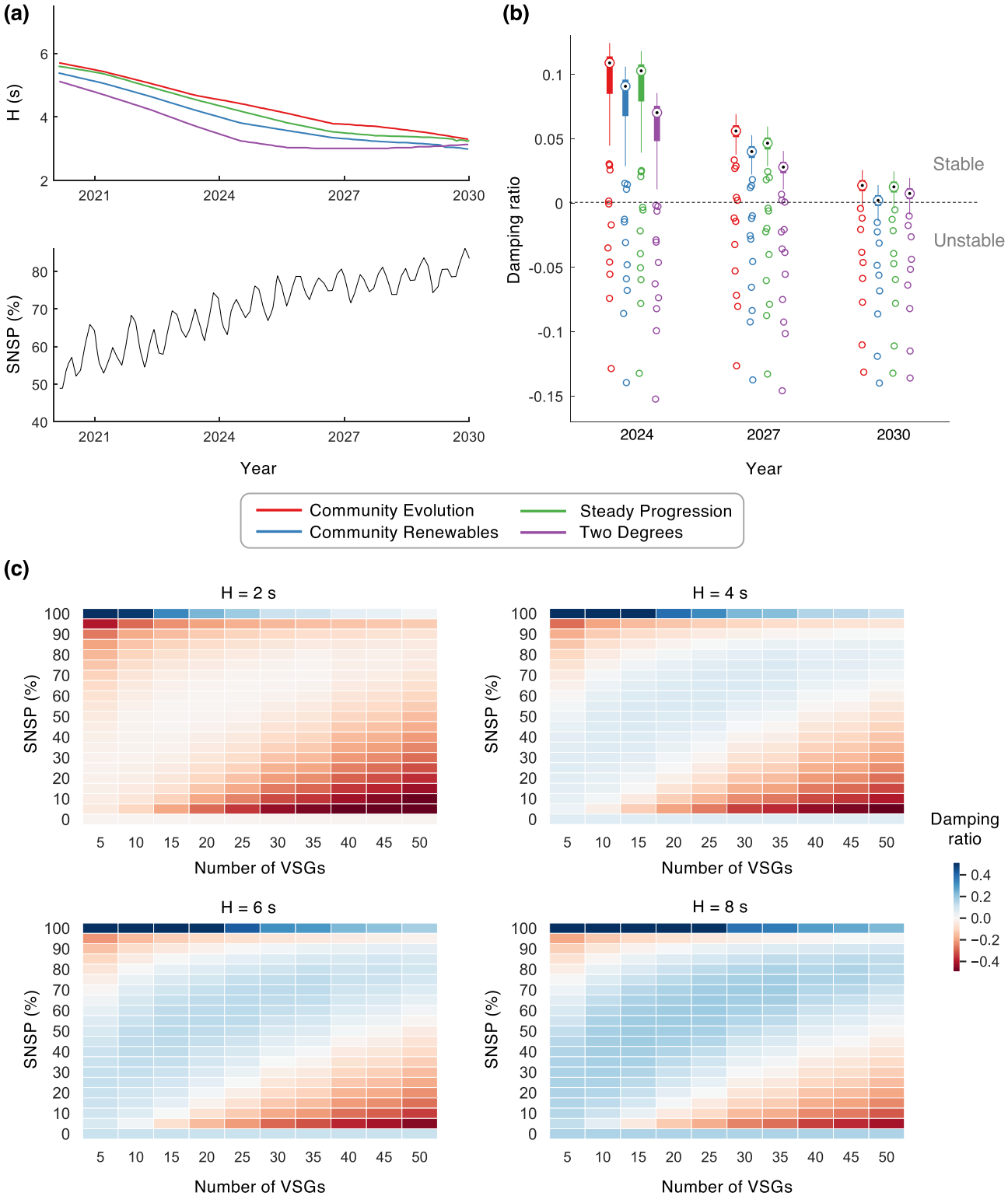

Figure 1. Small-signal instability in the Greater London power grid for various energy futures considering virtual synchronous generators. (**a**) Projections of the mean system inertia constant, *H*, for four future energy scenarios and the system non-synchronous penetration (SNSP) (Source: National Grid[39,40]). (**b**) Distributions of the damping ratio for the projected grid in 2024, 2027, and 2030. We assume 30 VSGs provide energy and inertia in addition to the currently-existing rotating synchronous generators. Results are shown for 100 simulations where the locations of the inverters were chosen randomly. The central mark, bottom, and top edges of each box plot represent the median, 25th, and 75th percentiles, respectively. Outliers are marked as individual circles. (**c**) Impact on the grid stability as the number of VSGs and SNSP change. Each cell in the heat maps is the average damping ratio over 100 simulations where the locations of the inverters were chosen randomly.

In practice, unstable grids experience generator and/or line trips from exceeding the voltage and/or frequency limits, resulting in blackouts.

The results of our analysis are summarized in Fig. 1b for three specific instances in the future. Here, we randomly vary the inverters' locations in the grid for each projected inertia and SNSP value, and depict the distribution of the resultant damping ratios in the box plot. Our results show that instabilities may arise when VSGs are introduced regardless of the future energy scenario—with the damping ratio worsening with reducing system inertia—underscoring the need to consider small-signal stability while designing pathways for the sustainability transition. We further study how the number of VSGs in the grid—a parameter whose value is uncertain in the future and could vary in real-time—impacts its stability, and whether increasing the overall system inertia can guarantee stability. Referring to Fig. 1c, two key observations can be gleaned from our simulations. First, the stability of the grid improves when the overall inertia is increased. Surprisingly however, we find that even with a fairly high inertia constant, say $H = 8$ s, the grid proves to be unstable for certain values of SNSP and number of VSGs, indicating that simply satisfying a minimum inertia criterion would be insufficient to guarantee the stability of the future power grid. Second, there exists a symmetry in each of the heat maps depicted in Fig. 1c—nearly along the anti-diagonal—resulting in two distinct regions of low stability. On closer examination, we find that instabilities worsen when there is a larger disparity between the capacities and therefore the droop gains of the different generators in the grid, be it virtual or rotating (see "Methods"). In the top-left of the heat maps, the latter contribute a very small fraction of the total generation capacity, and consequently, have high droop gains. In contrast, in the bottom-right corner, VSGs supply the smaller fraction, and have high droop gains. These high-droop-sources exhibit more aggressive control actions, and consequently, unstable behavior. Further, in the bottom-right, the stability worsens as the number of VSGs increases. The addition of more inverters for the same SNSP value not only increases their individual droop gains, but also reduces the effective electrical distance between any pair of inverters; this increases the feedback gain for the inverters' controllers, further reducing the stability. In the first and last rows of the heat maps, the higher-droop-sources are entirely eliminated, resulting in higher stability and the discontinuity seen in the damping trends. Commenting on the above observations, the symmetry along the anti-diagonal is reflective of the similarity between VSGs and rotating synchronous generators. Given the fact that the former were developed precisely to mimic the latter, there is no qualitative distinction between the two in our analysis. Overall, our results show that for every inertia and SNSP value, there exists an upper limit on the number of VSGs that can stably coexist in the system—this limit increases with the inertia. For example, assuming an inertia constant of 4 s and SNSP = 50%, we find that the Greater London grid can support, at a maximum, 35 VSGs, and for 6 s, 40 VSGs. When the number of VSGs is further increased, the bottom instability region takes over the entire SNSP range at some point; this limit also increases with inertia. The above observations have implications for selecting the optimal number of grid-forming inverters for varying power systems and energy futures.

External interventions for stability improvement. Presently, some power grids utilize external stabilizing grid-following converters to damp out oscillations, e.g., using wind farms[42]. Here, we apply the same principle for the VSG grid under study, and examine whether an additional VSG can be added to the grid to stabilize it. To this end, we consider three randomly-chosen unstable scenarios for the Greater London grid—see Fig. 2a—where in each, there are 10 VSGs in addition to the currently existing synchronous generators. The respective damping ratios are shown in Fig. 2b. Intuitively, a newly-added inverter can provide the highest possible stability if it behaves as an *infinite bus* with zero droop coefficients, contributing infinite inertia[43]. (This would also be mathematically identical to adding a high-capacity rotating synchronous generator instead.) On performing the stability analysis with the additional VSG, we find that the damping ratio for each scenario either remains the same or slightly decreases. Given that an infinite bus—arguably the most stable VSG configuration—cannot mitigate the instability, our results indicate that external interventions such as the addition of new stabilizing generators may not be beneficial to improve the small-signal stability. Instead, we hypothesize that the instability can be successfully mitigated if the existing inverters themselves participate in the stabilization process. Preferably, they would respond in a *decentralized* manner, i.e., only use information available locally and not rely on real-time instruction from the grid operator; this would enable the control philosophy to be scalable to larger grids.

Stability storage analogue for energy storage. We have already shown that the stability is affected by the network topology, generators' locations, sizes, and primary controller parameters (inertia constant and damping factor; see "Methods"). Of these, generator locations and sizes are generally fixed for a particular system, and for synchronous generators, as are the primary controller parameters (although power system stabilizers[44] can be enabled, if existing, to improve the damping factor). For VSGs, while the inertia and damping factor can in general be independently tuned, combining the requirements of inertia and energy sharing result in the damping factor not being able to be independently changed, as it directly influences the steady-state active power output. Therefore, the only parameters that can be potentially changed are the network impedances that interconnect the various generators. Intuitively, a solution to the instability problem is to increase the impedance between the inverters, as this reduces the feedback gain. While the physical power lines connecting the inverters cannot be changed in practice, one can however change the *effective impedance* between them by suitably modifying the inverter control scheme. More specifically, this could be achieved by the inverters emulating an additional impedance at their outputs—see Fig. 3a—which is popularly called virtual impedance control in the literature[27,28].

In this paper, we develop an adaptive mechanism for exploiting the virtual impedance control strategy in a decentralized fashion through the stability market where inertia is also traded. Central to this is to view the

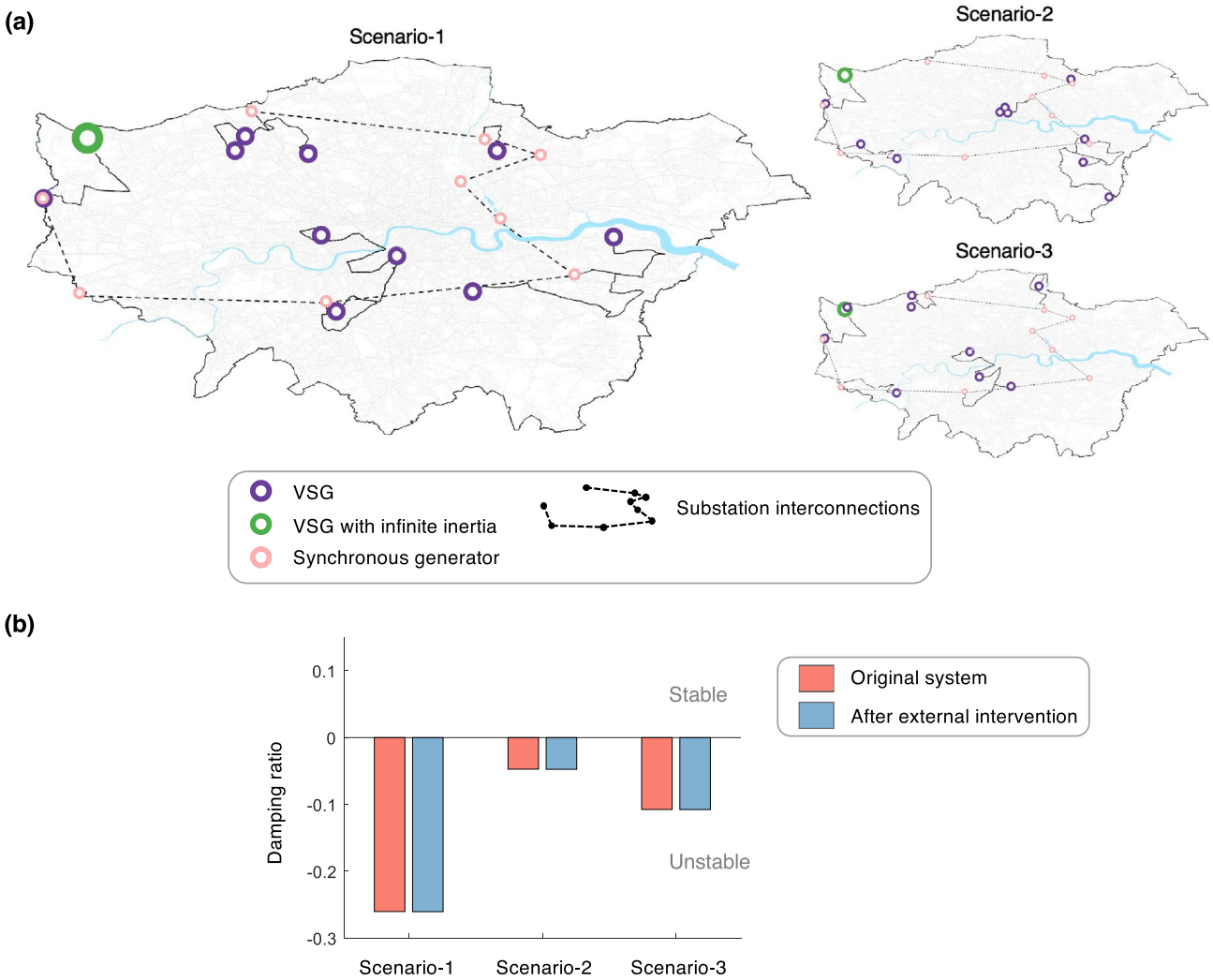

Figure 2. Demonstrating how external interventions may not guarantee stability of the future grid. (**a**) The figure presents three scenarios where 10 VSGs share the load with the existing rotating synchronous generators. In each scenario, a new VSG, marked in green, is added to provide infinite inertia in an exaggerated attempt to stabilize the grid. (**b**) Damping ratios of the scenarios in (**a**) before and after the external intervention, showing no improvement in stability.

output impedance of a VSG as *stored stability* in the inverter, which may be contributed to the grid when needed. This is directly analogous to how energy storage devices provide stored energy when it is not available from other sources, e.g., intermittent renewable generation[45]; see Table 1. Energy storage devices function by providing power, within their capacity, to the grid until the generation deficit is compensated fully. Equivalently, a stability storage device should contribute output impedance until it compensates for the instability introduced by the addition of inverter(s) to the grid.

The challenge remains to quantify the contribution of each stability storage device and the corresponding incentive due to it. While an energy storage device is compensated for the amount of the instantaneous power capacity and overall energy that it provides, in the stability analogue, the contribution of each participant is interlinked and not immediately separable as the overall system stability (quantified by the damping ratio) is a global property. Therefore, we propose a metric, termed as *distributed stability metric* (DSM) that can capture the individual contribution of each VSG to the overall stability, see Fig. 3b and "Methods". Note that different nodes have different interconnection impedances and VSGs with different controller parameters, and as a result, contribute varying amounts to the (in)stability. When a new inverter is added, the DSM quantifies how much instability this addition contributes to the grid, and also how much *additional* stability storage must be added to maintain stability. The latter can be contributed by a single inverter (e.g., the newly-added inverter), and/or by other existing inverters. The incentive offered for this grid service is directly proportional to the contributed stability, i.e., the change in the DSM before and after an inverter participates in this service. Referring to Fig. 3b, by the very design of the DSM, there is an upper limit on the improvement in stability versus the emulated impedance; this is in turn reflected in the incentive as well, see "Methods". In practice, the DSM can be calculated for each inverter using only locally measurable parameters and reported to the grid operator for obtaining monetary

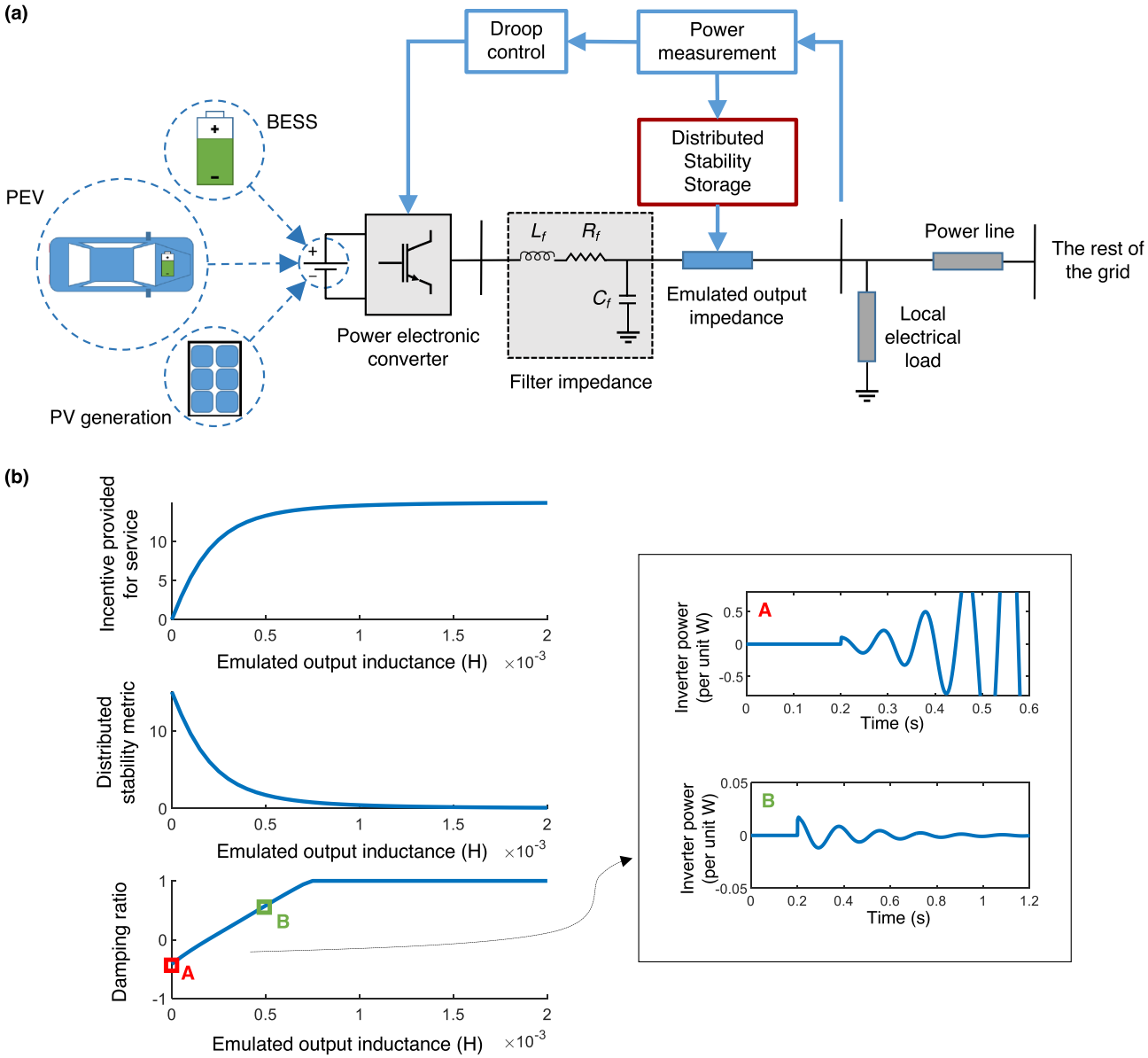

Figure 3. How VSGs can stabilize the power grid by performing as what we call *stability storage*. (**a**) Schematic of a VSG connected to the grid. The energy source could be a battery, electric vehicle, or renewable generation. The VSG emulates a virtual impedance to contribute stability storage to the grid. (**b**) Illustrating how the proposed distributed stability metric and damping ratio of the VSG vary as the emulated output inductance increases. The incentive for providing stability storage is simply the negative of the distributed stability metric, offset to be always positive. The insets on the right present the time responses of the system to a small load disturbance at 0.2 s. [BESS: Battery Energy Storage System, PEV: Plug-in Electric Vehicle, PV: Photovoltaic].

	Energy storage	Stability storage
Capability	Bridge the generation–demand gap due to intermittency of stochastic generation	Contribute additional impedance to maintain stability amongst interacting generators
Rewarded quantity	Power capacity and energy contributed	Improvement in the DSM
Nature of control	Decentralized, can be provided as a distributed service	Decentralized, can be provided as a distributed service
Potential participants	Any prosumer with a battery or other storage connected to the grid	Any prosumer operating a VSG

Table 1. Analogy between energy storage and stability storage.

compensation for the service, similar to energy metering. Multiple stability storage devices can participate in a decentralized manner simultaneously; this additivity is important to giving prosumers the freedom whether to participate in this grid service or not. Ultimately, the goal is to delegate and empower prosumers that benefit from providing energy and inertia to the grid to also be responsible for its small-signal stability.

Leveraging stability storage for stabilizing VSGs. We now take up the three unstable scenarios from Fig. 2a and demonstrate how the stability storage functionality stabilizes them. We begin with Scenario-1. While the system is unstable, interestingly, we find that the instability occurs only when one particular VSG, marked as 'Inv-1' in Fig. 4a, is present in the grid; see Fig. 4b,c. This is in part due to its close proximity to a neighboring synchronous generator 'SG-1'. We now demonstrate how the proposed stability storage service enables Inv-1 to be stably added to the grid. Referring to Fig. 4b, the system damping falls from 0.0756 to $-0.2602 < 0$ when Inv-1 is connected; this damping change can be detected locally by the inverters through power measurements. Subsequently, all inverters, including the newly added one, contribute additional output impedance, what we call stability storage. The particular contributions of each inverter vary according to their location, but the goal is to bring each DSM below a desired threshold; see "Methods" and Fig. 4d. With stability storage, the damping ratio becomes $0.1232 > 0$, or, the grid becomes stable. We find similar outcomes for Scenarios-2 and -3 as well.

Next, in cognizance of the likelihood that not all prosumers/inverters would be willing to participate in the stability storage service, we vary the fraction of inverters that do participate and analyze the stability of the Greater London grid considering 30 VSGs. For the purposes of this analysis, we assume that each participating VSG contributes the same amount of output impedance to the grid. The distribution of the damping ratios obtained over 100 simulations—where the locations of the inverters change randomly—are presented in Fig. 5. (Supplementary Note S1 presents the same results for different values for the number of VSGs, inertia, and SNSP.) Here, we make two observations: (i) the improvement in the stability is higher when more VSGs participate as stability stores, and when the magnitude of impedance contributed by each is higher; and (ii) the more the penetration of stability storage, the lower the impedance needed to ensure stability across a wide range of scenarios. These behaviors can be attributed not only to the additive property of stability storage, but also the fact that certain inverters contribute more towards instability than others (e.g., see Inv-1 in the case study from Fig. 4a). Therefore, stored stability available from or near these inverters is more impactful in recovering the damping than those farther away. As such, the more inverters that provide the stability storage service, the more the chance of an opportune inverter being available to provide much-needed output impedance.

Overall, the stability storage functionality can be leveraged to ensure stability of the Greater London grid for all energy futures shown in Fig. 1b; see Fig. 6a. As for the heat maps presented in Fig. 1c, Fig. 6b shows the same results with stability storage. While the majority of scenarios now become stable, we comment on the negative damping ratios observed at the top-left. As was mentioned previously, the instability here arises from the high droop gains of the small-capacity synchronous machines. Our results show that this cannot be addressed by interventions from the VSGs (along the same lines as external interventions in Fig. 2), and must necessarily be mitigated by phasing out these synchronous generators—this is evident from the top row of the heat maps where the damping ratios are all positive.

Methods

Power grid specifications. The power grid topology of the Greater London area used in this study was obtained using (i) electric substation data from National Grid, the UK transmission grid operator[46]; and (ii) road network and building data from OpenStreetMap[47]. From the former, we obtain the list of the nine 400 kV/230 kV substations that feed the Greater London distribution grid. From the latter, we obtain the list of buildings in the city, which constitute the loads in the grid. Subsequently, based on the reasonable assumption that distribution lines are usually laid alongside roads, we derive the power grid topology as a set of spanning trees that connect the nine substations to the loads closest to them; see ref.[48] for more details and Supplementary Note S2 for the resultant topology. Within each subnetwork, the distribution lines are classified into eight different tiers, with the lines closest to the substations or laid alongside larger roadways assigned as Tier-0, and the ones serving the leaf nodes or laid alongside smaller roads assigned as Tier-7. The values of the line impedances were approximated based on typical R/X ratios and impedance per length values for each tier; see Supplementary Note S2. As for inertia requirements shown in Fig. 1a, we use projections from National Grid[39] for the total system inertia (in GVA s) for four future energy scenarios[41], which we divide by the total capacity of synchronous generation (in GVA) obtained from the Government of UK[49] to obtain the system inertia constant H (in s). To obtain the SNSP projections presented in Fig. 1a, we subtract from 100% the projected contribution of synchronous generation that we obtain from Ref.[40]. While validation of the distribution grid used for our analyses is clearly not possible due to the unavailability of details of the actual grid, we draw comfort by anchoring the following to reality: (i) the locations and number of the substations that feed the grid; (ii) that distribution lines follow the road network; and (iii) the inertia requirements according to the UK grid operator. On another note, the substations in our study are represented by generic and equivalent synchronous generators, allowing our analyses to be agnostic to diverse types of generation plants and energy mixes that feed the transmission network.

Modeling virtual synchronous generators. Various models for VSGs have been put forth in the literature[22–26]. In its most fundamental form, a VSG is controlled to emulate the swing equation of a rotating synchronous generator that relates the active power output P to the frequency f of the output voltage:

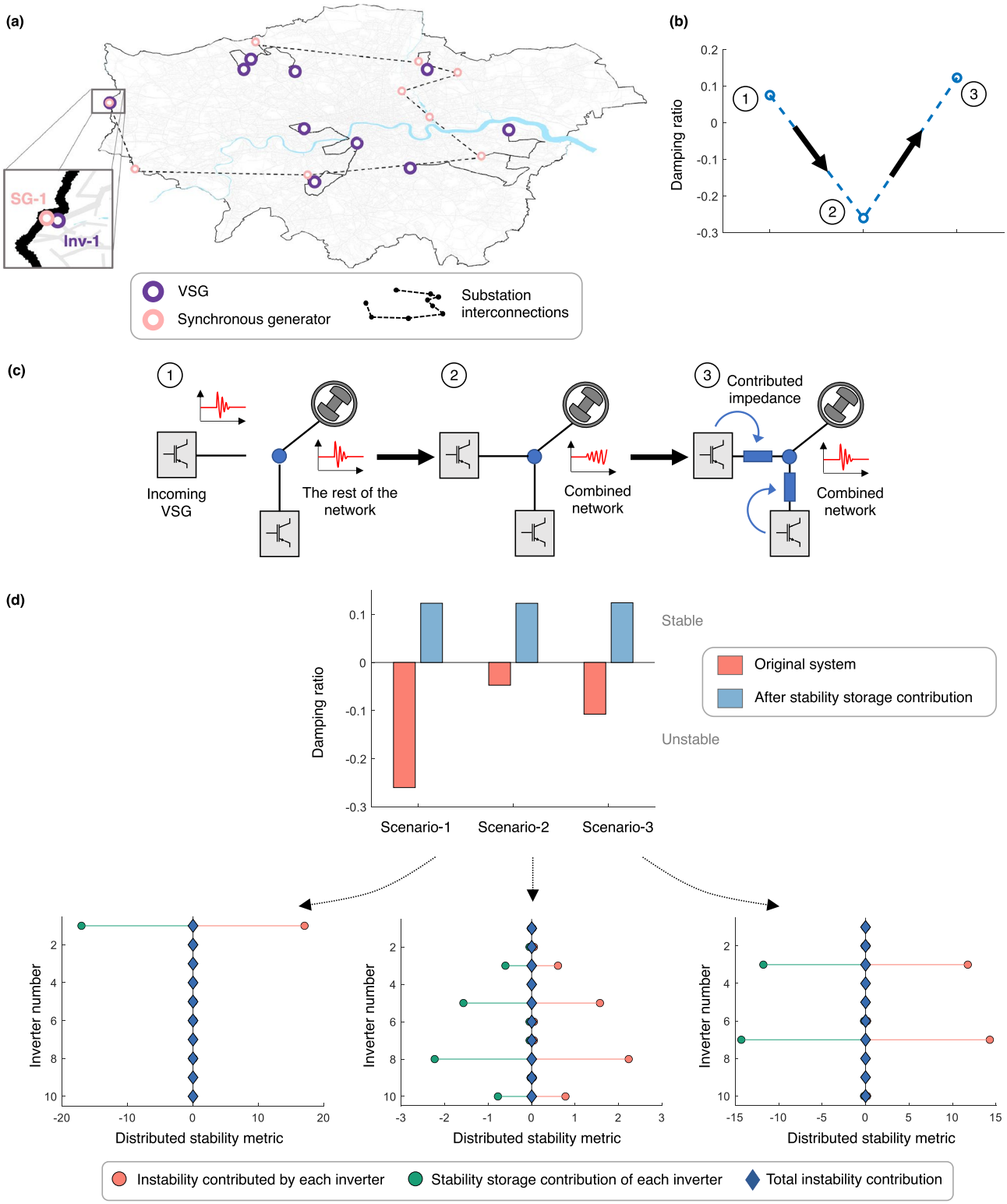

Figure 4. Using VSGs as stability stores to expand inverter-based generation in the power grid. (**a**) Location of the rotating and virtual synchronous generators in Scenario-1 from Fig. 2, showing the addition of a new VSG, named Inv-1. (**b**) Damping ratio in (**a**) before and after the addition of Inv-1. Also shown is the damping ratio after all VSGs contribute stability storage. (**c**) Illustrating how a new VSG can be added to the grid while preserving stability. The following sequence is depicted: an incoming VSG is to be added to a stable grid; the combined network becomes unstable as a result; and the combined network regains its stability after the VSGs participate as stability stores. (**d**) Damping ratio for the three unstable scenarios in Fig. 2 before and after all inverters provide stability storage. Also shown is the contribution of each inverter to the instability of the grid, and the effect of stability storage in mitigating the respective instability contributions. The incentive provided to each inverter for its service is proportional to the stability storage contributed.

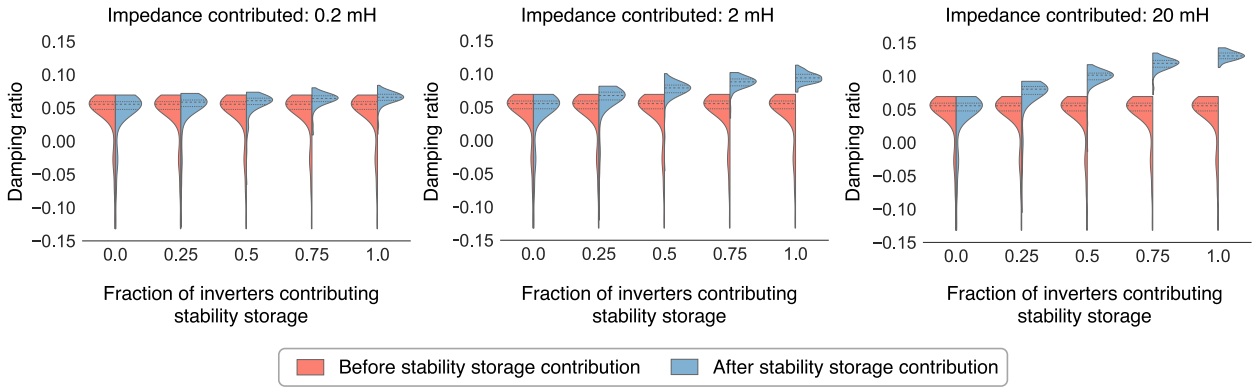

Figure 5. Varying the VSG participation in the stability storage service. Damping ratio before and after stability storage contribution with a varying fraction of inverters participating in this service. Results are presented over 100 simulations in which there are 30 VSGs randomly located across the network. Three results are shown when the impedance contribution of each inverter varies as 0.2 mH, 2 mH, and 20 mH. The system inertia constant H is maintained at 4 s, with SNSP set at 80%. Each pod of the violin plot depicts the quartiles of the respective distributions.

$$f = f_0 - \frac{1}{2Hs + D}P \tag{1}$$

where f_0 is the nominal value of the frequency, H the inertia constant, and D the damping factor. As the power output of the inverter changes, the frequency changes as well, contributing inertia and damping to the dynamic response. This also enables the sharing of power amongst multiple sources in the grid, as the frequency changes in relation with the active power drawn with the steady-state slope k_f, termed as the frequency droop coefficient:

$$k_f = \frac{1}{D}, \tag{2}$$

and the first-order time constant:

$$T_c = \frac{2H}{D}. \tag{3}$$

To enable reactive power sharing, a voltage droop is employed, which changes the output voltage reference V_{ref} in relation to the reactive power Q drawn from the inverter:

$$V_{ref} = V_0 - \frac{k_v}{T_c s + 1}Q, \tag{4}$$

where V_0 is the nominal voltage and k_v the voltage droop gain.

The overall control scheme for the inverter is cascaded, with the outputs from the VSG controller being fed to a voltage controller that tracks the reference V_{ref}, and finally a current controller and sinusoidal pulse-width modulator that generate the switching inputs for the inverter. Detailed control diagrams are presented in Supplementary Note S3. In our simulations, we consider $f_0 = 50$ Hz. The value of V_0 depends on the voltage level of the inverter, i.e., it depends on the tier of the distribution line to which it is connected; see Supplementary Note S2. The cut-off frequency $1/(2\pi T_c)$ of the VSG dynamic response is typically selected between 2 and 10 Hz[43], taken here as 2 Hz.

Stability analysis. We perform stability analysis in the frequency domain using MATLAB. We do not use time domain simulations as the goal here is to assess the small-signal stability of the grid rather than observing its transient behavior during instabilities. The transition from conventional generation to fully inverter-based generation is characterized by the SNSP. If S_{total} is the total power demand in the system and S_{sg1},S_{sg2},$\cdots$,S_{sgi},$\cdots$,$S_{sgN_{sg}}$ and S_1,S_2,$\cdots$,S_j,$\cdots$,$S_{N_{inv}}$ are the powers supplied by the synchronous generators $i \in [1, N_{sg}]$ and inverters $j \in [1, N_{inv}]$, respectively, we define:

$$SNSP = \frac{\sum_{j=1}^{N_{inv}} S_j}{S_{total}} \tag{5}$$

where $S_{total} = \sum_{i=1}^{N_{sg}} S_{sgi} + \sum_{j=1}^{N_{inv}} S_j$. We now detail how the power system is modeled, and how the stability is assessed for each SNSP value. For each of the synchronous generators, their relative power capacities β_i are modeled to be proportional to the number of buildings connected to that spanning tree:

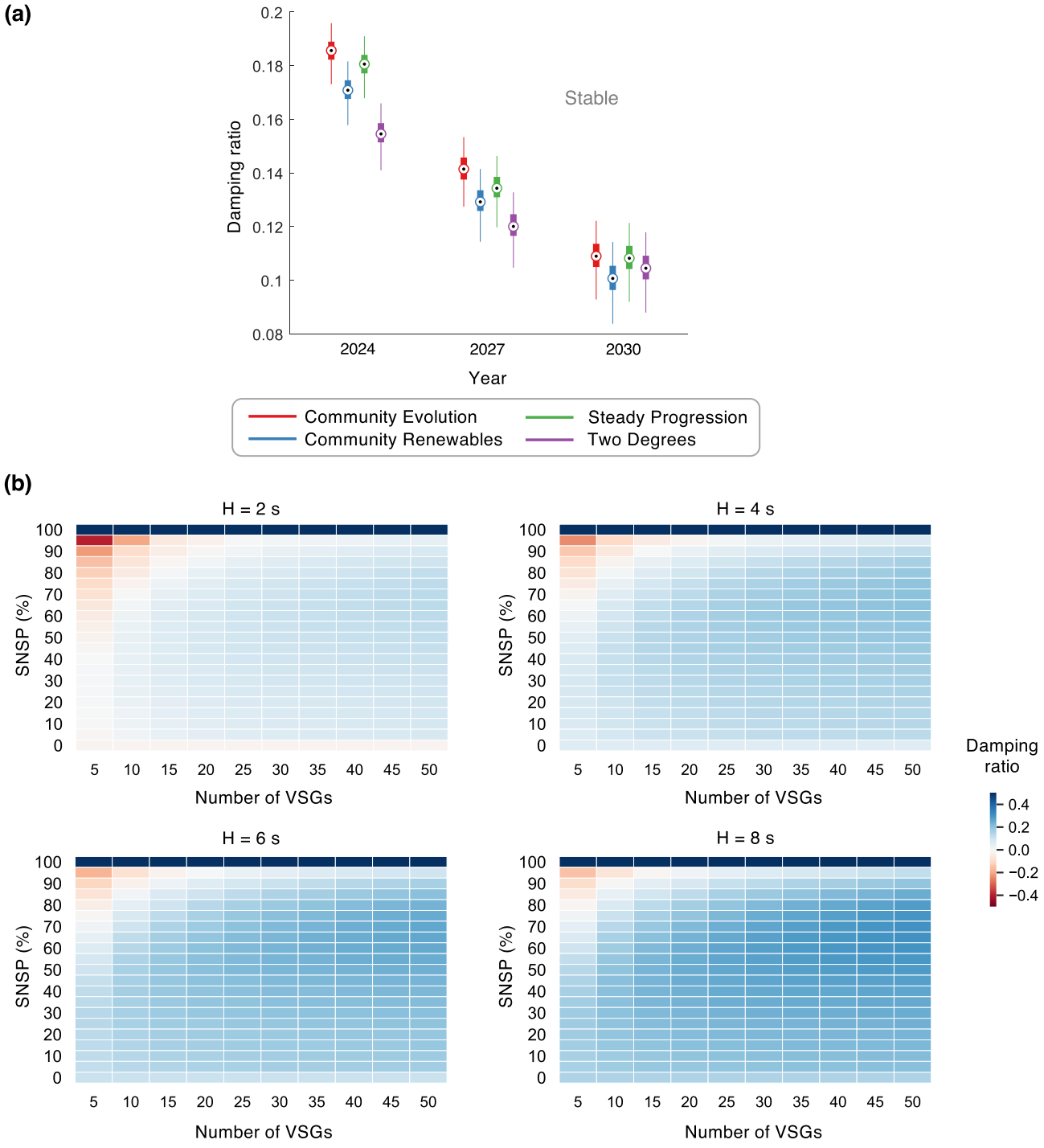

Figure 6. Effectiveness of stability storage in the Greater London grid for various energy futures. How the stability of the projected grids in (**a**) Fig. 1b, and (**b**) Fig. 1c changes when all VSGs participate as stability stores. The central mark, bottom, and top edges of each box plot in (**a**) represent the median, 25th, and 75th percentiles, respectively.

$$\beta_i = \frac{\text{Number of buildings connected to spanning tree } i}{\text{Total number of buildings}}. \tag{6}$$

We assume for simplicity that the inverters are of equal capacity. Then, for a given value of SNSP, considering the total system capacity S_{total} to be constant, the power capacities of the synchronous generators and inverters are calculated as:

$$S_{sgi} = \beta_i S_{total}\ (1 - SNSP)\ \forall i \in [1, N_{sg}] \tag{7}$$

$$S_j = S_{total} \frac{SNSP}{N_{inv}} \ \forall j \in [1, N_{inv}] \tag{8}$$

In this study, we do not simulate the inertia market to determine the inertia contributions by each source. Rather, we consider that the grid operator fixes the overall required inertia, and that each source contributes an inertia proportional to its capacity. Given the power capacity S_i of a generic generation unit and its inertia constant H_i, overall inertia of the system H_{total} is given by:

$$H_{total} = \frac{\sum_i^{N_{sg}+N_{inv}} H_i S_i}{S_{total}} \tag{9}$$

Then, the inertias H_i to be contributed by the $n = N_{sg} + N_{inv}$ sources are:

$$\begin{bmatrix} H_1 \\ H_2 \\ H_3 \\ \vdots \\ H_n \end{bmatrix} = \begin{bmatrix} S_1 & S_2 & S_3 & \dots & S_n \\ S_2 & -S_1 & 0 & \dots & 0 \\ S_3 & 0 & -S_1 & \dots & 0 \\ \vdots & & & \ddots & \\ S_n & 0 & 0 & \dots & -S_1 \end{bmatrix}^{-1} \begin{bmatrix} S_{total} H_{total} \\ 0 \\ 0 \\ \vdots \\ 0 \end{bmatrix} \tag{10}$$

Subsequently, the other parameters of the VSG controllers are calculated as:

$$D_i = \frac{2H_i}{T_c} \tag{11}$$

$$k_{vi} = r_0 \frac{T_c}{2H_i} \tag{12}$$

where r_0 is the ratio of the voltage droop gain to the frequency droop gain, selected here as 3. Note that droop gains are expressed in per unit Hz/per unit W or per unit V/per unit VAR, with the per unit conversion done on a common frequency and power base; these are taken as 50 Hz and 10 GVA for our simulations respectively. The voltage base depends on the voltage of the line where the source is situated.

For each iteration of our simulations, the locations of the inverters are randomly selected from nodes that are connected with either Tier-1 or Tier-2 lines. More formally, if $\mathcal{E}$ is the set of all edges in the network, the set of potential nodes for locating the inverters is given by $\mathcal{S} = \{\cup s_i : \mathcal{E}(s_i) \in \{\text{Tier-1, Tier-2}\}\}$ where $\mathcal{E}(s_i)$ refers to the set of edges connected to the node s_i in the network. Then, the bus admittance matrix of the power network is obtained by eliminating all nodes that do not have an active source (either a VSG or a synchronous generator) through Kron reduction. The poles of the system are then identified; see Supplementary Note S4 for a detailed description. Of the system poles, the complex pole-pair that has the maximum real part is defined as the dominant mode of oscillation; the damping ratio of this pair is used to determine if the grid is stable. We remark here that the system has a null eigenvalue denoting the freedom to shift the reference of all the voltage phasor angles, which is neglected.

Note that for the heat maps in Figs. 1c and 6b, when SNSP is 0, the inverters are all removed from the model altogether, and when SNSP is 100%, the synchronous machines are all removed. Otherwise, the model considering both would produce undefined results as the droop gains of the sources tend to infinity when their power shares tend to zero. This discontinuity in the model results in the observed discontinuity in the damping ratio trends in the first and last rows of the heat maps.

Distributed stability metric. We define the following as the distributed stability metric:

$$\text{DSM} = \frac{\omega_c k_f}{2} \left[B' - \frac{2k_v G' G}{1 - k_v B} + \frac{k_v G^2 (1 - \omega_c k_v B')}{\omega_c (1 - k_v B)^2} \right], \tag{13}$$

where $\omega_c = \frac{1}{T_c}$ is the cut-off frequency of the power measurement filter in the inverter, representative of the inertia. Further, G and B represent the real and imaginary parts of the static admittance (i.e., the inverse of the impedance) connecting the inverter to a Thévenin-equivalent of the rest of the grid, respectively. G' and B' are the real and imaginary parts of the dynamic admittance that captures the transient behavior of the interconnection impedance[50]. From a control theoretic perspective, the DSM reflects the distance of the dominant pole-pair—pertaining to a system where the inverter is connected to an infinite bus that approximates the rest of the grid—from the origin. Therefore, the metric for a given VSG is independent from the parameters of the other VSGs in the grid, thereby allowing us to separate the (in)stability contribution of each. For more details on its derivation, see Supplementary Note S5. Selection of this metric has the following benefits: (i) it can be calculated locally at each VSG node without any information from the others; and (ii) it varies intuitively, taking the value of 0 when the VSG is located at an infinite electrical distance from the rest of the grid (i.e., when $G = B = G' = B' = 0$, it does not affect the grid stability at all), and monotonically increasing as the electrical distance reduces (i.e., when G, B, G', and B' increase). When a VSG contributes stability storage, its effective output impedance to the grid becomes larger and more inductive (which are the conditions for improved stability); the metric decreases and finally saturates at 0, e.g., see Fig. 3b. Finally, we define the incentive/payoff for the prosumer operating the VSG as follows: 0 when the inverter contributes no emulated output impedance, and proportionally increasing

with the reduction in the DSM, saturating at a maximum when the metric saturates at 0. A VSG participating as a stability store operates as follows. It continually measures the damping ratio of its power output, e.g., through Prony analysis[51]. If the damping ratio falls below a preset threshold, here zero, the inverter contributes additional output impedance (see Supplementary Note S3 for detailed control diagrams) until its individual instability contribution decreases to a small value, taken in our study as 0.001. We remark here that the output impedance should not be increased beyond the value needed to compensate instability, as it would adversely impact the ability of the generator to provide reactive power and respond to dynamic load changes.

Conclusion

Different grids around the world have different decarbonization pathways and generation mixes. As such, their inertia and SNSP futures are different. Our study helps energy policymakers and power utilities from diverse power systems to develop a viable roadmap towards achieving higher VSG and therefore renewable penetrations. To begin, we have shown that there is an optimal number, and an upper limit in the number of grid-forming inverters or VSGs that can be present in the grid while maintaining its small-signal stability. Additionally, our results demonstrate that recruiting VSGs with smaller capacities jeopardizes the stability of the grid. Given these constraints, operators can contract prosumers of suitable capacities to participate in forming the grid and providing inertia through the stability market, so that the number VSGs remains below the limit. Yet, despite such long-term planning by the utilities, the number of VSGs operating can change in the short-term depending on, e.g., generation stochasticity, changing prosumer needs, faults, or other failures. Then, the stability storage service proposed in this paper can enable the robust operation, while adequately compensating the prosumers for this additional service. The prosumers continue to provide stability storage as a stop-gap measure until grid-level coordination obviates its need by calling for an increase in the overall inertia from prosumers, bringing online generators of higher capacity, removing generators with smaller capacities, or effecting updates on primary controller parameters through secondary control. Meanwhile, the secondary control structure can also be utilized to tackle the side-effects arising from implementing the stability storage functionality such as voltage sag and changing reactive power share due to the changes in the VSGs' output impedance. On another note, the stability storage concept can be adapted and extended through future studies to scalably address phenomena other than small-signal stability in inverter-dominated grids, e.g., voltage or harmonic stability.

Finally, our paper has implications on standards development pertaining to inverter-based generation in bulk power systems. Existing standards such as IEEE 1547[52] (active standard for distribution grids) and IEEE P2800 (draft standard for transmission grids)[53] detail requirements only for grid-following inverters, given that there exist no grid-forming inverters in bulk grids at present. With the introduction of grid-forming inverters such as VSGs imminent, requirements for these are presently under consideration[4], e.g., the GC0137 standard being developed by National Grid in the UK[54]. Our paper directly informs these deliberations by pointing out the need to include stabilizing functions such as variable output impedance in addition to the inertia and droop functions.

Data availibility

The power systems data used for the analyses are available at Ref.[55].

Code availability

The codes for generating the specific plots are available from the corresponding author upon request.

Received: 9 February 2022; Accepted: 20 July 2022
Published online: 12 August 2022

References

1. Yang, W. *et al.* Burden on hydropower units for short-term balancing of renewable power systems. *Nat. Commun.* **9**(1), 1–12 (2018).
2. National Renewable Energy Laboratory. Inertia and the power grid: a guide without the spin. https://www.nrel.gov/docs/fy20osti/73856.pdf, 2020.
3. Uriarte, F. M., Smith, C., Vanbroekhoven, S. & Hebner, R. E. Microgrid Ramp Rates and the Inertial Stability Margin. *IEEE Trans. Power Syst.* **30**(6), 3209–3216 (2015).
4. Lin, Y., Eto, J. H., Johnson, B. B., Flicker, J. D., Lasseter, R. H., Villegas, P., Hugo, N, Seo, G.-S., Pierre, B. J., & Abraham, E. Research roadmap on grid-forming inverters. Technical report, National Renewable Energy Lab.(NREL), Golden, CO (United States) (2020).
5. National Grid ESO. The potential operability benefits of virtual synchronous machines and related technologies. https://www.nationalgrideso.com/document/168376/download, 2020. Accessed on: 31/08/2021.
6. European Network of Transmission System Operators for Electricity. High penetration of power electronic interfaced power sources and the potential contribution of grid forming converters (2020).
7. National Grid ESO. Markets roadmaps to 2025. https://www.nationalgrideso.com/document/188666/download (2021). Accessed on: 31/08/2021.
8. Xie, L., Singh, C., Mitter, S. K., Dahleh, M. A., & Oren, S. S . Toward carbon-neutral electricity and mobility: Is the grid infrastructure ready? *Joule* **5**(8), 1908–1913 (2021).
9. Zhang, Y., Xie, L. & Ding, Q. Interactive control of coupled microgrids for guaranteed system-wide small signal stability. *IEEE Trans. Smart Grid* **7**(2), 1088–1096 (2016).
10. Stephan, A., Battke, B., Beuse, M. D., Clausdeinken, J. H. & Schmidt, T. S. Limiting the public cost of stationary battery deployment by combining applications. *Nat. Energy* **1**(June), 16079 (2016).
11. Gao, C., Liu, X. & Chen, H. Research on the control strategy of distributed energy resources inverter based on improved virtual synchronous generator. *Sci. Rep.* **7**(1), 1–12 (2017).
12. Aderibole, A., Zeineldin, H. H, El-Moursi, M. S., Peng, J.C.-H., Al Hosani, M. Domain of stability characterization for hybrid microgrids considering different power sharing conditions. *IEEE Trans. Energy Conversion* **33**(1), 312–323 (2017).
13. Nikolakakos, I. P., Al-Zyoud, I. A., Zeineldin, H. H., El-Moursi, M. S., & Al-Hinai, A. S. Enhancement of islanded droop-controlled microgrid performance via power filter design. In *IEEE Power Energy Society General Meeting*, (October):4–8 (2014).

14. Pagnier, L. & Jacquod, P. Inertia location and slow network modes determine disturbance propagation in large-scale power grids. *PLoS ONE* **14**(3), e0213550 (2019).
15. Menck, P. J., Heitzig, J., Kurths, J., & Schellnhuber, H. J. How dead ends undermine power grid stability. *Nat. Commun.* **5**(1), 1–8 (2014).
16. Simpson-Porco, J. W., Dörfler, F., & Bullo, F. Voltage collapse in complex power grids. *Nat. Commun.* **7**(1), 1–8 (2016).
17. Motter, A. E, Myers, S. A, Anghel, M., Nishikawa, T. Spontaneous synchrony in power-grid networks. *Nat. Phys.* **9**(3), 191–197 (2013).
18. Tyloo, M., Pagnier, L., & Jacquod, P. The key player problem in complex oscillator networks and electric power grids: Resistance centralities identify local vulnerabilities. *Sci. Adv.* **5**(11), eaaw8359 (2019).
19. Molnar, F., Nishikawa, T., & Motter, A. E. Asymmetry underlies stability in power grids. *Nat. Commun.* **12**(1), 1–9 (2021).
20. Hellmann, F. *et al.* Network-induced multistability through lossy coupling and exotic solitary states. *Nat. Commun.* **11**(1), 1–9 (2020).
21. Dörfler, F., Chertkov, M. & Bullo, F. Synchronization in complex oscillator networks and smart grids. *Proc. Natl. Acad. Sci.* **110**(6), 2005–2010 (2013).
22. Khan, M. A. U., Hong, Qi., Liu, D., Egea-Àlvarez, A., Avras, A., Dyśko, A., Booth, C., & Rostom, D. Experimental assessment and validation of inertial behaviour of virtual synchronous machines. *IET Renew. Power Gen.* (2022).
23. Suvorov, A., Askarov, A., Kievets, A. & Rudnik, V. A comprehensive assessment of the state-of-the-art virtual synchronous generator models. *Electric Power Syst. Res.* **209**, 108054 (2022).
24. Rathnayaka, A. J. D., Potdar, V. M., Dillon, T., Hussain, O. & Kuruppu, S. Goal-oriented prosumer community groups for the smart grid. *IEEE Technol. Soc. Mag.* **33**(1), 41–48 (2014).
25. Zhang, B. & Zhang, J. Small-signal modeling and analysis of a three-phase virtual synchronous generator under off-grid condition. *Energy Rep.* **8**, 1200–1207 (2022).
26. Cheema, K. M., Chaudhary, N. I., Tahir, M. F., Mehmood, K., Mudassir, M., Kamran, M., Milyani, A. H, & Elbarbary, Z. M. S. Virtual synchronous generator: Modifications, stability assessment and future applications. *Energy Rep.* **8**, 1704–1717 (2022).
27. He, J. & Li, Y. W. Analysis, design, and implementation of virtual impedance for power electronics interfaced distributed generation. *IEEE Trans. Ind. Appl.* **47**(6), 2525–2538 (2011).
28. Wang, X., Li, Y. W., Blaabjerg, F., & Loh, P. C. Virtual-impedance-based control for voltage-source and current-source converters. *IEEE Trans. Power Electron.* **30**(12), 7019–7037 (2014).
29. Yajuan, G., Guerrero, J. M., Xin, Z., Vasquez, J. C., & Xiaoqiang, G. A new way of controlling parallel-connected inverters by using synchronous-reference-frame virtual impedance loop-part i: Control principle. *IEEE Trans. Power Electron.* **31**(6), 4576–4593 (2015).
30. Po-Hsu, H., Petr, V., Mohamed, A. H., Kirtley, J. L., Konstantin, T. Plug-and-play compliant control for inverter-based microgrids. *IEEE Trans. Power Syst.* **34**(4), 2901–2913 (2019).
31. Raman, G. & Peng, J. C.-H. Mitigating stability issues due to line dynamics in droop-controlled multi-inverter systems. *IEEE Trans. Power Syst.* **35**(3), 2082–2092 (2020).
32. Dheer, D. K., Vijay, A. S., Kulkarni, O. V., & Doolla, S. (2019) Improvement of stability margin of droop-based islanded microgrids by cascading of lead compensators. *IEEE Trans. Ind. Appl.* **55**(3), 3241–3251.
33. De Brabandere, K. *et al.* A voltage and frequency droop control method for parallel inverters. *IEEE Trans. Power Electron.* **22**(4), 1107–1115 (2007).
34. Raman, G., Peng, J. C.-H. & Zeineldin, H. H. Optimal damping recovery scheme for droop-controlled inverter-based microgrids. *IEEE Trans. Smart Grid* **11**(4), 2805–2815 (2020)
35. Parag, Y., & Sovacool, B. K. Electricity market design for the prosumer era. *Nat. Energy* **1**(4) (2016).
36. Babazadeh, M. & Nobakhti, A. Robust decomposition and structured control of an islanded multi-dg microgrid. *IEEE Trans. Smart Grid* **10**(3), 2463–2474 (2018).
37. Al kez, D., Foley, A. M, McIlwaine, N., Morrow, D. J., Hayes, B. P., Zehir, M. A., Mehigan, L., Papari, B., Edrington, C. S., & Baran, M. A critical evaluation of grid stability and codes, energy storage and smart loads in power systems with wind generation. *Energy* **205**, 117671 (2020).
38. Bottrell, N., Prodanovic, M. & Green, T. C. Dynamic stability of a microgrid with an active load. *IEEE Trans. Power Electron.* **28**(11), 5107–5119 (2013).
39. National Grid ESO. Operating a low inertia system: a system operability framework document. https://www.nationalgrideso.com/document/164586/download, 2020. Accessed on: 31/08/2021.
40. Gomersall, B. National Grid ESO–operability & future inertia trends. https://www.era.ac.uk/write/MediaUploads/EPRI%20Presentations/Talk_5_-_National_Grid_ESO_-_National_Grid_ESO_Operability_and_Future_Inertia_Trends.pdf, Accessed on: 30/08/2021. (2020)
41. National Grid ESO. Future energy scenarios. https://www.nationalgrideso.com/document/170756/download, 2019. Accessed on: 31/08/2021.
42. Wang, Y., Meng, J., Zhang, X. & Xu, L. Control of PMSG-based wind turbines for system inertial response and power oscillation damping. *IEEE Trans. Sustain. Energy* **6**(2), 565–574 (2015).
43. Mohamed, Y. A. R. I., & El-Saadany, E. F. Adaptive decentralized droop controller to preserve power sharing stability of paralleled inverters in distributed generation microgrids. *IEEE Trans. Power Electron.* **23**(6), 2806–2816 (2008).
44. Ghosh, A., Ledwich, G., Malik, O. P., & Hope, G. S. Power system stabilizer based on adaptive control techniques. *IEEE Trans. Power Apparat. Syst.* **PAS-103**(8), 1983–1989 (1984).
45. Ziegler, M. S., Mueller, J. M., Pereira, G. D., Song, J., Ferrara, M., Chiang, Y.-M., & Trancik, J. E . Storage requirements and costs of shaping renewable energy toward grid decarbonization. *Joule* **3**(9), 2134–2153 (2019).
46. National Grid ESO. Appendix c-power flow diagrams, electricity ten year statement 2017. https://www.nationalgrideso.com/document/101736/download.
47. OpenStreetMap. www.openstreetmap.org.
48. Raman, G., AlShebli, B., Waniek, M., Rahwan, T., & Jimmy, C. H. P. How weaponizing disinformation can bring down a city's power grid. *PLOS ONE* **15**(8), e0236517 (2020).
49. Martin, V. Digest of UK energy statistics (DUKES): electricity, chapter 5. https://assets.publishing.service.gov.uk/government/uploads/system/uploads/attachment_data/file/1006701/DUKES_2021_Chapter_5_Electricity.pdf. Accessed on: 31/08/2021. (2021)
50. Vorobev, P., Huang, P.-H., Al Hosani, M., Kirtley, J. L., & Turitsyn, K. High-fidelity model order reduction for microgrids stability assessment. *IEEE Trans. Power Syst.* **33**(1), 874–887 (2017).
51. Peng, J. C.-H., & Nair, N. Comparative assessment of Kalman filter and Prony methods for power system oscillation monitoring. In: 2009 IEEE Power and Energy Society General Meeting, pp. 1–8 (2009).
52. IEEE. IEEE standard for interconnection and interoperability of distributed energy resources with associated electric power systems interfaces. IEEE Std 1547-2018 (Revision of IEEE Std 1547-2003), pp. 1–138 (2018).
53. IEEE. IEEE draft standard for interconnection and interoperability of inverter-based resources (IBR) interconnecting with associated transmission electric power systems. IEEE P2800/D6.1, June 2021, pp. 1–197, 2021.

54. National Grid ESO. GC0137: Minimum Specification Required for Provision of GB Grid Forming (GBGF) Capability (formerly Virtual Synchronous Machine/VSM Capability). https://www.nationalgrideso.com/industry-information/codes/grid-code-old/modifications/gc0137-minimum-specification-required, 2021. Accessed on: 31/08/2021.
55. Raman, G., AlShebli, B., Waniek, M., Rahwan, T., & Peng, J. C.-H. How weaponizing disinformation can bring down a city's power grid: Supplementary data. https://www.penglaboratory.com/topology-data, (2019).

Acknowledgements
The research was conducted at the Future Resilient Systems at the Singapore-ETH Centre, which was established collaboratively between ETH Zurich and the National Research Foundation Singapore. This research is supported by the National Research Foundation Singapore (NRF) under its Campus for Research Excellence and Technological Enterprise (CREATE) programme. This work was also supported by the Singapore Ministry of Education Academic Research Fund Tier-1 grant A-8000214-01-00. The authors gratefully acknowledge the assistance provided by Dr. Marcin Waniek, New York University, Abu Dhabi, UAE in generating the map-based plots in the paper.

Author contributions
R.G.P., R.G.R., and J.C.-H.P. conceived the study. R.G.P. and R.G.R. generated the figures and performed the analyses. All authors wrote the manuscript.

Competing interests
The authors declare no competing interests.

Additional information
Supplementary Information The online version contains supplementary material available at https://doi.org/10.1038/s41598-022-17065-7.

Correspondence and requests for materials should be addressed to J.C.-H.P.

Reprints and permissions information is available at www.nature.com/reprints.

Publisher's note Springer Nature remains neutral with regard to jurisdictional claims in published maps and institutional affiliations.